PNAS

Supplementary Information for
The Mechanism for Ligand Activation of the GPCR-G-Protein Complex

Amirhossein Mafi, Soo-Kyung Kim, and William A. Goddard III*

* corresponding author
Email: wag@caltech.edu

This PDF file includes:

1. Methods

1.1. Gq Protein-First activation mechanism of 5-HT_{2A}- serotonin receptor and Gq protein

To model the pre-coupled complex of 5-HT_{2A}-Gq protein, we used the inactive conformation(*1*) of 5-HT_{2A} (PDB ID: 6WH4) resolved by X-ray crystallography and added the 45 missing residues, ^{266}L-M^{311}, comprising the intracellular loop (ICL3), to the protein structure. Subsequently, we optimized the ICL3 with the MODELLER program(*2*) and chose an extended conformation that does not clash with the Ras-like domain of the Gαq subunit.

To predict the heterotrimeric Gq protein-bound GDP which comprises: Gαq, Gβ, and Gγ, we used the crystal structure(*3*) of heterothermic Gi protein bound with GDP (PDB ID: 1GOT)(*4*), as a template to perform homology modeling using the MODELLER program(*2*). The Gi protein was chosen because of a reasonably high sequence similarity (>~60%) between these two heterotrimeric G proteins. Eventually, the Gα-α5 helix was optimized by placing intra-helical hydrogen bond restraints with a force constant of ~1.4 kcal.mol^{-1}Å^{-2}. To make a pre-coupled complex, we separately aligned Gαq (Gαq-α5 helix and Ras-like domain), Gβ, Gγ, and inactive 5-HT_{2A} to corresponding protein chains/segments in the fully active state complex of 5-HT_{2A}-$G_{\alpha q,\beta,\gamma}$ (PDB ID: 6WHA (*1*)) respectively. Needleman-Wunsch alignment (*5*) algorithm with BLOSUM-62 matrix was used for the superimposition which are incorporated in UCSF Chimera(*6*). The distance between N (i+4) and C(i) atoms of the residues in all α-helices, hereafter inter-helical hydrogen bond restraints, were restrained at a distance of 4.1 Å with a force constant of ~1.4 kcal.mol^{-1}Å^{-2}. Finally, the refined 5-HT_{2A} and our modeled Gq protein-bound GDP were separately aligned to the fully active[3] state (PDB ID: 6HWA) of 5-HT_{2A}, and Gq protein. Then, we aligned the 5-HT_{2A} to the 'orientation of proteins in membranes' (OPM) structure to immerse the complex into the palmitoyl-oleoyl-phosphatidylcholine (POPC) membrane bilayer and water. We embedded the aligned complex in the POPC membrane using CHARMM-GUI interface(*1*, *7*).

After a short MD equilibration (described below), to evaluate the energetics of Gq pre-coupling to 5-HT_{2A}, we carried out a metaD simulation for ~400 ns (Table S1) in which we applied bias forces on key variables, describing interactions between Gαq-α5 helix and the cytoplasmic region of 5-HT_{2A}:

i) a salt bridge between V358 (C) and R173$^{3.50}$(CZ)
ii) a salt bridge between K353 (NZ) and E318$^{6.30}$(CD)

We repeated our metaD free energy calculations for ~600 ns (Table S1) to independently assess the energetics of ionic lock opening upon the binding of Gq protein by Adding a third variable:

iii) a salt bridge between R173$^{3.50}$(CZ)and E318$^{6.30}$(CD)

To exclude the possibility that the specific rigid-body orientation of Gq protein led to emergence of pre-coupled state between 5-HT_{2A}-Gq, we independently modeled a pre-coupled state in which we included only the Gαq-α5 peptide (the last 26 residues: ^{333}T-V^{358}) and placed it in close proximity (K353 and V358 10Å away from R173$^{3.50}$ and E318$^{6.30}$, respectively) to the inactive 5-HT_{2A}. Then, to follow our G Protein-First mechanism of activation, we performed a ~1.5 μs metaD free energy calculations (Table S1) on which we evaluated the energetics relevant to the following interactions:

i) a salt bridge between V358 (C) and R173$^{3.50}$(CZ)
ii) a salt bridge between K353 (NZ) and E318$^{6.30}$(CD)
iii) a salt bridge between R173$^{3.50}$(CZ) and E318$^{6.30}$(CD)

To determine the role of different types of ligands in our G Protein-First mechanism of activation, and to find how different types of ligands promote the pre-coupled 5-HT_{2A}-Gq protein-GDP complex to the fully active state, we inserted:

i) a full agonist, 25CN-NBOH to the pre-coupled complex using the binding site of the cryo-EM (PDB ID: 6WHA) active structure(*1*)
ii) a partial agonist, LSD, to the pre-coupled complex using the binding site of the X-ray crystallographic (PDB ID: 6WGT) structure(*1*)
iii) an inverse agonist, methiothepin, to the pre-coupled complex using the binding site of the X-ray crystallographic (PDB ID: 6WH4) structure(*1*)

We found that the extracellular portion of 5-HT_{2A} aligns very well between our pre-coupled 5-HT_{2A}-Gq state and: 1) the crystallographic inactive (PDB ID: 6WH4)(1), with r.m.s.d. of 1.8 Å in the binding pocket, 2) partially active (PDB ID: 6WGT)(1), with r.m.sd. of 1.2 Å in the binding pocket, and (3) fully active structure (PDB ID: 6WHA)(1) with r.m.sd. of 1.1 Å in the binding pocket, allowed us to insert ligands into our pre-coupled 5-HT_{2A}-Gq complex. We used Needleman-Wunsch alignment (*5*) algorithm with BLOSUM-62 matrix for the superimposition, which are incorporated in UCSF Chimera(*6*). We performed 1 ns (20 cycles) of simulated annealing, in which the system was first heated from 25 to 600 K over 20ps with a sequence of 25, 100, 310, 450, 600 K and then sharply cooled back to 310K over 30 ps. In this calculation, we placed harmonic restraints on backbone atoms with a force constant of ~6.0 kcal.mol^{-1}Å^{-2}, while the side chains were free to find the optimum conformation. Subsequently, we embedded this pre-minimized liganded-5-HT_{2A}-Gq-GDP complex into a membrane bilayer composed of ~350 POPC molecules (Table S1) in a simulation box of $110\times110\times167$ Å^3. We solvated this simulation box with water and ions to neutralize the system and added 0.15M NaCl, leading to ~206,000 atoms in the calculations.

We also studied a case with no ligand present at the orthosteric binding pocket of 5-HT_{2A} to evaluate energetics relevant to constitutive activity. After short MD equilibrations (see below), we performed metaD simulations (~ 1 μs on aggregate) to evaluate the energetics relevant to activation in the presence of ligands. In our free energy calculations, we estimated the energetics of:

1) opening the Gαq-bound GDP from its inactive structure with the GDP bound between the AH and Ras subdomains: the distance between AH domain [the center of mass of Cα for the residues 154-161 and 175-182] and Ras-like domain [the center of mass of Cαs for the residues 51-62]

2) repacking the cytoplasmic region of 5-HT_{2A} due to the presence of ligand and Gq protein:

i) The distance between TM3 [the center of mass of Cα for residues 168-178] and TM6 [the center of mass of Cα for residues 318-328]
ii) The distance between TM6 [the center of mass of Cα for residues 318-328] and TM7 [the center of mass of Cα for residues 372-382]
iii)

Following the previous calculations, we equilibrated our optimized 25CN-NBOH-5-HT_{2A}-Gq-GDP complex for a ~430 ns to characterize the fully activated state. However, we imposed several upper and lower walls on several key variables during these calculations to discourage the Gαq-α5 from exploring the previous inactive states:

1) an upper wall at a distance of 23.0 Å between TM6 [the center of mass of Cα for residues 318-328] and Gαq-α5 helix [the center of mass of Cα for residues 330-354] with a force constant ~1.2 kcal.mol^{-1}Å^{-2}.

2) an upper wall at a distance of 26.0 Å between TM5 [the center of mass of Cα for residues 253-263] and Gαq-α5 helix [the center of mass of Cα for residues 330-354] with a force constant ~1.2 kcal.mol^{-1}Å^{-2}.

3) an upper wall at a distance of 30.0 between Gαq-α4 helix [the center of mass of Cα for residues 275-283] and a loop on Gα [the center of mass of Cα for residues 329-36] with a force constant ~1.2 kcal.mol^{-1}Å^{-2}.

4) an upper wall at a distance of 79.0 Å along the z-axis between Gαq-α5 helix [the center of mass of Cα for residues 330-354] and the surface origin (0,0,0) with a force constant ~1.2 kcal.mol^{-1}Å^{-2}.

5) a lower wall at a distance of 23.0 Å along the x-axis between Gαq-α5 helix [the center of mass of Cα for residues 330-354] and the surface origin (0,0,0) with a force constant ~24.0 kcal.mol^{-1}Å^{-2}.

6) a lower wall at a distance of 23.0 Å between AH domain [the center of mass of Cα for the residues 154-161 and 175-182] and Ras-like domain [the center of mass of Cαs for the residues 51-62] with a force constant ~24.0 kcal.mol^{-1}Å^{-2}.

We also placed a set of harmonic restraints with a force constant of ~24.0 kcal.mol^{-1}Å^{-2} on the distances of:

i) TM3-TM6 at a distance of 14.0 Å
ii) TM6-TM7 at a distance of 17.2 Å
iii) TM3-TM5 at a distance of 10.8 Å
iv) TM5-TM6 at a distance of 10.5 Å

1.2. Gs Protein-First activation mechanism of β2-adrenergic receptor and Gs protein

We started with the crystal structure (PDB ID: 2RH1)(*8*) to model the inactive state of β2-adrenergic receptor (β_2AR). In this crystal structure, the ICL3 had been replaced with the fusion T4 lysozyme (T4L) protein to stabilize the basal activity of inactive β_2AR to facilitate crystallization. Unexpectantly, the resolved structure features a moderate hydrophobic interaction between R131$^{3.50}$ and L272$^{6.34}$ rather than a strong charge-charge interaction between E268$^{6.30}$-R131$^{3.50}$. Thus, to characterize the inactive conformation of β_2AR regarding its TM3-TM6 coupling, we first removed the ligand and then optimized the inactive conformation in two different ways:

1) β_2AR-T4L
2) β_2AR-ICL3

For the β_2AR-ICL3, we first minimized the β_2AR-T4L using metaD simulations(*9*) for ~600 ns (Table S2). Subsequently, we used the optimized structure of β_2AR-T4L to replace the T4L with the native residues 231-262, constituting the ICL3. We added an extended conformation of ICL3 and optimized it with MODELLER program(*2*). Here, we included the β_2AR lipid modification in our calculations by modeling in palmitoyl-cysteine 341. We immersed both β_2AR-T4L and β_2AR-ICL3 into the POPC membrane, water, and ions, which results in a simulation box of 103×103×102 Å^3 with ~110,000 atoms.

After a short equilibration, to optimize the inactive conformation of the .β_2AR structure, we performed well-tempered metaD(*9*) simulations to assess the energetics of a microswitch from:

1) a hydrophobic interaction between R131$^{3.50}$(CG) and L272$^{6.34}$(CD2); to
2) a strong charge-charge interaction between E268$^{6.30}$(CD) and R131$^{3.50}$(CZ)

We continued the metaD simulation to attain convergence of the free energy profiles. In this study, we monitored the free energy difference between two relevant local minima with time until

the energy difference ceased changing noticeably with time (the fluctuations in the uncertainty dampened significantly to less than ~1 kcal/mol).

To follow our G Protein-First activation paradigm, we started with the inactive-β_2AR (exhibiting the ionic lock between TM3-TM6) and coupled it to inactive Gs protein-bound GDP. To bind inactive Gs protein to the receptor, we used a geometry and orientation similar to the Gs protein in the fully active state complex(*10*) (PDB ID: 3SN6) resolved by X-ray crystallography. Thus, we separately superimposed our optimized β_2AR-ICL3 and inactive Gαs, Gβ, and Gγ, to corresponding protein chains in the fully active state complex of -β_2AR -Gs (PDB ID: 3SN6) respectively. Needleman-Wunsch alignment (*5*) algorithm with BLOSUM-62 matrix was used for the superimposition which are incorporated in UCSF Chimera(*6*). To model the inactive state of the Gs protein, we used the crystal structure of Gαs-bound GDP (PDB ID: 6AU6)(*11*). We then added the Gαs-αN helix, residues 1-38, relevant to the short isoform of Gαs by superimposing this structure to the Gαs subunit of the crystal structure of β2-Gs complex (PDB ID: 3SN6)(*12*). We reconstructed several side chains using Swiss-pdbviewer(*13*) that were not fully resolved. Then, we modeled in the Gαs subunit palmitoyl-cysteine 3 into the structure. Thus, we included the first 9 residues of the Gαs-αN helix. Subsequently, the added Gαs-αN and Gαs-α5 helices were optimized while placing intra-helical hydrogen bond restraints with a force constant of ~1.4 kcal.mol^{-1}Å^{-2}. To prepare the Gs heterotrimer-bound GDP complex, we started with the G$\beta\gamma$ subunit from the crystal structure of β_2-Gs-agonist complex (PDB ID: 3SN6)(*12*).

Then, we performed 10 ns (200 cycles) of simulated annealing, in which the system was first heated from 25 to 600 K over 20ps with a sequence of 25, 100, 310, 450, 600 K and then sharply cooled back to 310K over 30 ps. In this calculation, we placed harmonic restraints on backbone atoms with a force constant of ~6.0 kcal.mol^{-1}Å^{-2}, while the side chains were free to find the optimum conformation. Subsequently, we embedded this pre-minimized β_2AR-Gs-GDP complex into a membrane bilayer composed of 277 POPC molecules in a simulation box of 103×103×156Å^3. We solvated this simulation box with water and ions to neutralize the system and added 0.15M NaCl, leading to ~167,000 atoms in the calculations.

After a short equilibration, we carried out a metaD simulation for ~800 ns (Table S2), in which we applied bias forces on key variables, describing interactions between Gαs-α5 helix and the cytoplasmic region of β_2AR:

i) a salt bridge between E392(CD) and R131$^{3.50}$(CZ)
ii) a salt bridge between R389 CZ) and E268$^{6.30}$(CD)
iii) a salt bridge between R385(CZ) between and E237$^{5.76}$(CD)

1.3 G protein pre-coupling to inactive class A GPCRs

To prepare various G proteins (Gi2, Go, and G11) for our calculations, we built homology modeling using UCSF Chimera(*6*). We used our refined model of Gi1 for preparing Gi2 and Go proteins and our predicted model of Gq protein for G11 protein (described above). To model inactive conformations of GPCRs, we used the X-ray crystallographic inactive states (see Table S4) as templates. We added the missing residues, particularly the native residues on the ICL3 to complete the structures. Subsequently, we optimized the ICL3 conformation using MODELLER program(*2*) and then chose extended conformations that do not clash with the Ras-like domain of Gα subunits. To assemble the GPCR-GP-GDP complex, we used available crystallographic or cryo-EM active complexes (see Table S3) as templates to separately superimpose GPCRs and G proteins. To make a pre-coupled complex, we separately aligned Gα (Gα-αN helix and Ras-like domain), Gβ, Gγ, and inactive GPCRs to corresponding protein chains in the fully active state complex (shown in Table S3) respectively. Needleman-Wunsch alignment (*5*) algorithm with BLOSUM-62 matrix was used for the superimposition which are incorporated in UCSF Chimera(*6*). During the superimposition process, we also refined the position of GαN helix. Finally, we included the lipid modifications in our calculations by modeling in: myristoyl-Gly 2 to Gαi1, myristoyl- glycine 2 and palmitoyl-cysteine 3 to Gαi2, myristoyl- glycine 2 and palmitoyl-cysteine 3 to Gαo, and

palmitoyl-cysteine 9-10 to G11 protein. Afterwards, we embedded our GPCR-GP-GDP complexes into a membrane bilayer composed of POPC molecules and solvated them with water and 0.15 M excessive NaCl at the physiological pH=7.4. Here, we aligned the class A GPCRs to the ‘‘orientation of proteins in membranes’ (OPM) structure for immersing the pre-coupled complexes into the POPC membrane bilayer and water box. We embedded the aligned complex in the POPC membrane using the CHARMM-GUI interface(*1*, *7*). Before proceeding with our free energy calculations, we performed short MD equilibrations (see below) to prepare these systems for metaD simulations.

1.4 Agonist activation of pre-coupled A_{2A}-Gs protein

To determine how the agonist shifts the pre-coupled A_{2A}-Gs protein-GDP complex to the fully active state, we used the cryo-EM structure of A_{2A}-bound NECA coupled with an engineered Gs protein (PDB ID: 6GDG) as the basis to replace the engineered Gs protein by an inactive Gs protein-bound GDP (as described above). To make a A_{2A}-NECA-Gs protein-GDP complex, we separately aligned Gαs (Gαs-αN helix and Ras-like domain), Gβ, Gγ to corresponding segments of an engineered Gs protein. Needleman-Wunsch alignment (*5*) algorithm with BLOSUM-62 matrix was used for the superimposition which are incorporated in UCSF Chimera(*6*). We then embedded the obtained A_{2A}-NECA-Gs protein-GDP complex into a membrane bilayer composed of 280 POPC/65 cholesterol molecules in a simulation box of $110\times110\times156$Å^3. We subjected the complex to optimize for 10 ns MD simulation before metaD free energy calculations (Table S4) using Charmm36m(*14*) force field.

1.5 Initiation of activation by Ligand-First mechanism of activation

1) 5-HT_{2A}-bound with 25CN-NBOH. We inserted a full agonist 25CN-NBOH to our refined inactive state of 5-HT_{2A} (described above). We found that the extracellular portion of 5-HT_{2A} aligns very well between the crystallographic inactive(*1*) (PDB ID: 6WH4) and active(*1*) structure (PDB ID: 6WHA). Thus, we used the cryo-EM binding pose(*1*) (PDB ID: 6WHA) for insertion of 25CN-NBOH. We first superimposed the 5-HT_{2A} from our inactive conformation on the fully active structure from the cryo-EM.

To optimize the interactions between 5-HT_{2A} and 25CN-NBOH, we performed 1ns (20 cycles) of simulated annealing, in which the system was first heated from 25 to 600 K over 20ps using the sequence of 25, 100, 310, 450, 600 K and then sharply cooled back to 310 K over 30 ps. In this calculation, we placed harmonic restraints on backbone atoms with a force constant of ~9.6 kcal.mol^{-1}Å^{-2}, while the side chains were free to find the optimum conformation. Subsequently, we embedded this 5-HT_{2A} -agonist into a membrane bilayer composed of 111 POPC molecules in a simulation box of $101\times101\times96$ Å^3. We solvated this simulation box with water and ions to neutralize the system and added an additional 0.15 M NaCl.

To examine if 25CN-NBOH induces the ionic lock to break open, we separately performed a ~1.3 μs metaD simulation (Table S5) to assess the energetics of:

i) R173$^{3.50}$(CZ)-E318$^{6.30}$(CD)
ii) R173$^{3.50}$(CZ)-A321$^{6.33}$(CB)

2) 5-HT_{2A}-bound with 25CN-NBOH derived from the fully active cryo-EM(*1*) structure

We superimposed the TM1 of active 5-HT_{2A} (PDB ID: 6WHA)(*1*) in the cryo-EM structure onto the TM1 of the inactive conformation of 5-HT_{2A} (PDB ID: 6WH4)(*1*) in order to build in the missing residues. Then, to model 5-HT_{2A}-bound 25CN-NBOH, we removed the mini-Gq protein from the cryo-EM structure. Subsequently, we immersed the resulting 5-HT_{2A}-25CN-NBOH complex into a 132 POPC membrane bilayer and solvated it with water and ions

To determine whether 25CN-NBOH can stabilize the widely open cytoplasmic region of 5-HT_{2A}, we carried out a ~2.5 μs metaD simulation (Table S5) after a short equilibration (described below), where we evaluated the energetics relevant to repositioning of TM6. Thus, we applied the bias forces on:

- The distance between TM3 [the center of mass of Cα for residues 168-178] and TM6 [the center of mass of Cα for residues 318-328]
- The distance between TM6 [the center of mass of Cα for residues 318-328] and TM7 [the center of mass of Cα for residues 372-382]

1.6 Short equilibration of GPCR-GP systems and force fields/algorithms for free energy calculations

To prepare systems for extensive metaD calculations, we followed up the following procedure to equilibrate the systems.

We carried out 5000 steps of steepest descent energy minimization to relax the lipid packing around the protein construct and to relax the protein complex. During this process, the positions of all heavy atoms of proteins/GDP/ligands were restrained with a force constant of ~9.6 kcal.mol^{-1}Å^{-2}. For POPC, we used position restraints with a force constant of ~2.4 kcal.mol^{-1}Å^{-2} on just the z-coordinate of heavy atoms so that the POPC could move freely along the xy- plane to find the appropriate packing around the protein. Subsequently, we performed a short NVT (~100 ps) followed by short NPT (~10 ns) simulations where we placed positional restraints on the heavy atoms with a force constant of 9.6 kcal.mol^{-1} Å^{-2}. In addition, we restrained the z-coordinate of the headgroups of POPC inside the membrane with a force constant of ~2.4 kcal.mol^{-1}Å^{-2}. Throughout the calculations, the restraints on the protein, GDP, ligands, and POPC were gradually reduced to 0 kcal.mol^{-1}Å^{-2}, which prepared the construct for the further energy minimization.

In simulations using the Amber force field, the protein was described using Amber14(*15*) and the parameters for POPC were borrowed from LIPID14(*15*). The force field parameters for all bonded and non-bonded interactions of BI167107, DAMGO, and morphine were obtained from the Generalized Amber force field(*16*) using ACPYPE(*17*) and Antechamber16(*18*). The partial charges for the ligands were assigned with the semi-empirical AM1-BCC model(*19*) as incorporated in USCF chimera(*6*). The GDP parameters were borrowed from a combination of the Amber force field and the Meagher et al. et al. study.(*20*, *21*) The TIP3P(*22*) model was used to describe the water.

For simulations using the ChARMM36m force field, the proteins, POPC, GDP, and ions were described using the Charmm36m(*14*) parameter set. Water was described using the TIP3P model. The ligand was parameterized using the ParamChem server(*23*, *24*).

In our well-tempered metaD(*9*) simulations, the temperature was maintained at 310K using a velocity-rescale(*25*) thermostat with a damping constant of 1.0 ps for temperature coupling and the pressure was controlled at 1 bar using a Parrinello-Rahman barostat algorithm(*26*) with a 5.0 ps damping constant for the pressure coupling. Semi-isotropic pressure coupling was used during this calculation. The Lennard-Jones cutoff radius was 10 Å, where the interaction was smoothly shifted to 0 after 10 Å. Periodic boundary conditions were applied to all three directions. The Particle Mesh Ewald algorithm(*27*) with a real cutoff radius of 10 Å and a grid spacing of 1.2 Å was used to calculate the long-range coulombic interactions. A compressibility of 4.5 ×10^{-5} bar^{-1} was used in the xy- plane and also for the z axis, to relax the box volume. In all the above simulations, water OH-bonds were constrained by the SETTLE algorithm(*28*). The remaining H-bonds were constrained using the P-LINCS algorithm(*29*). All simulations were carried out using GROMACS(*30*) and metaD calculations were done using PLUMED-2(*31*). To expedite the sampling process, we imposed inter-helical hydrogen bonds restraints on affected helices during the simulations to avoid protein unfolding.

2. Figures

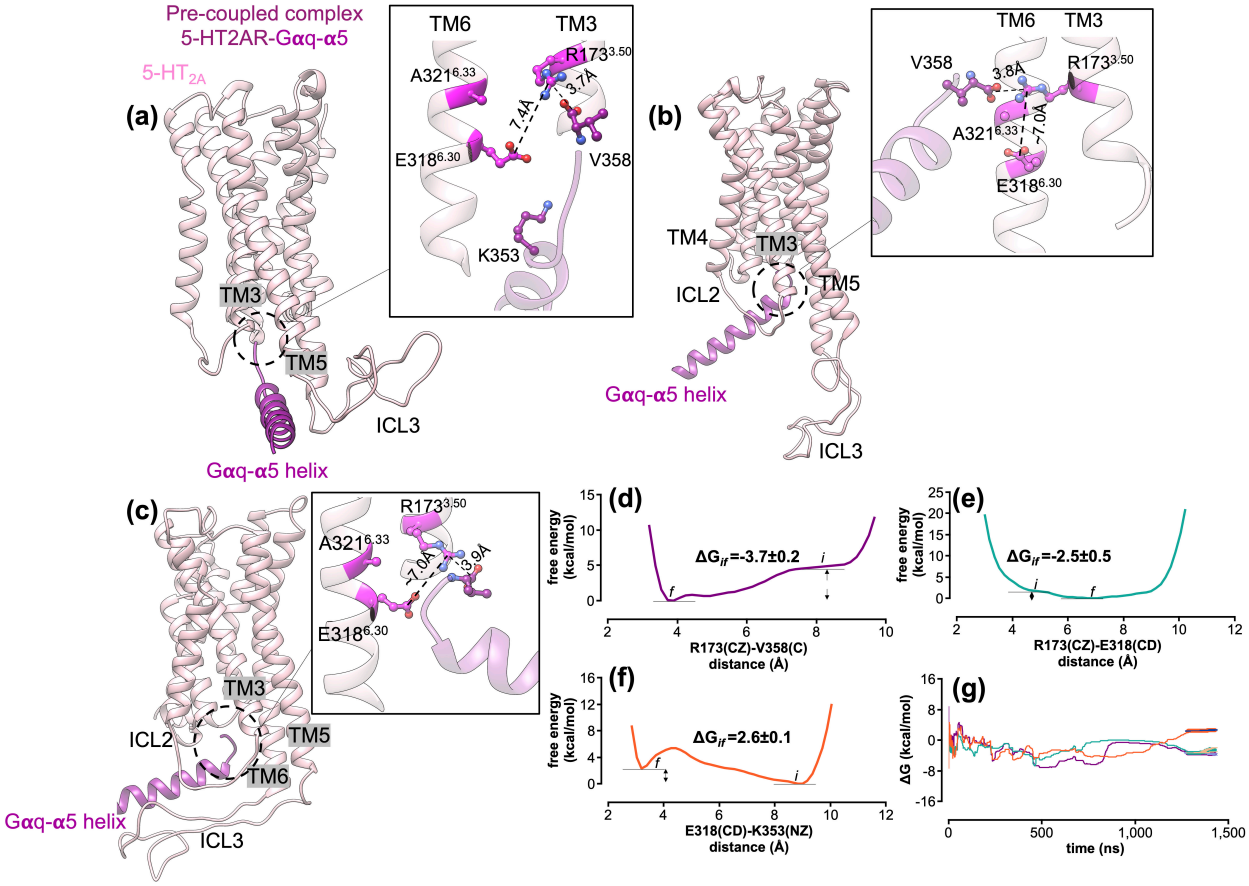

Figure S1. The pre-coupled complex of 5-HT$_{2A}$ and the Gαq-α5 peptide (the rest of the Gq protein was eliminated). (a)-(c) optimized interactions between Gαq-α5 peptide and cytoplasmic region of 5-HT$_{2A}$ for different conformations in the pre-coupled state complex. metaD free energy of **(d)** R173$^{3.50}$(CZ)-V358(C), R173$^{3.50}$(CZ)- E318$^{6.30}$(CD), and **(e)** E318$^{6.30}$(CD)- K353(NZ). **(g)** The variation of the free energy difference with time was calculated to monitor the free energy convergence. The weighted averages and the standard deviations (shown by blue, orange, and red bands in (**g**)) were calculated for the converged period.

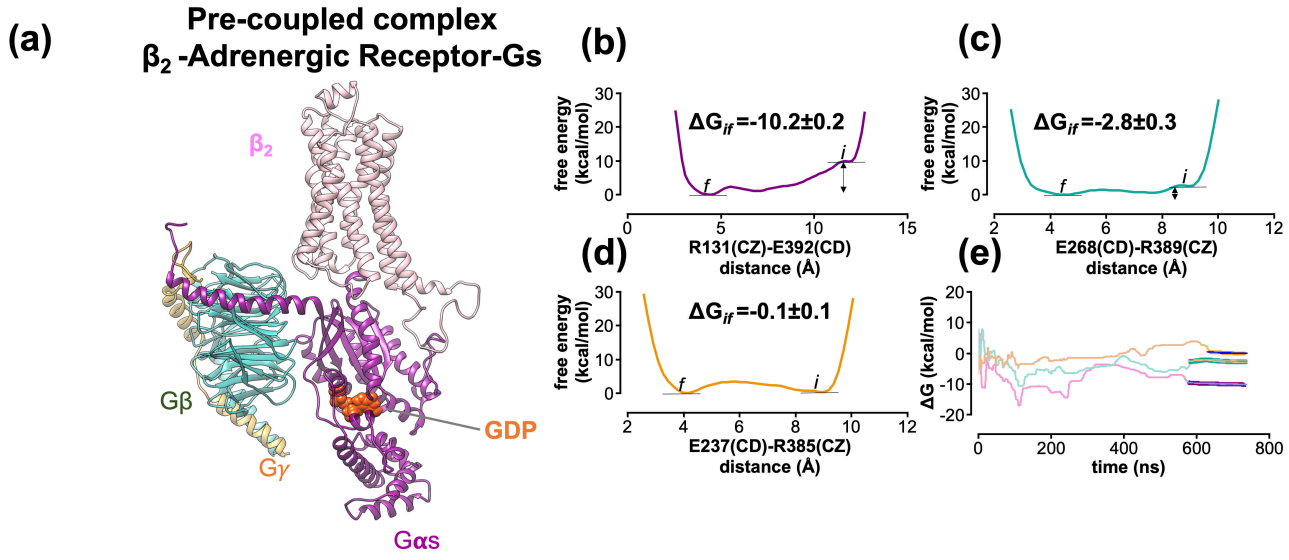

Figure S2. Sequence of the activation process for β_2 adrenergic receptor and Gs protein according to the G Protein-First activation mechanism. **(a)** pre-coupled complex formation between β_2 adrenergic receptor- Gs protein before ligand binding **(b-d)** metaD free energy calculations for the key collective variables (as also described in Table S2). **(e)** The variation of the free energy difference with time was calculated to monitor the free energy convergence. The weighted averages and the standard deviations (shown by blue, orange, and red bands were calculated for the converged period.

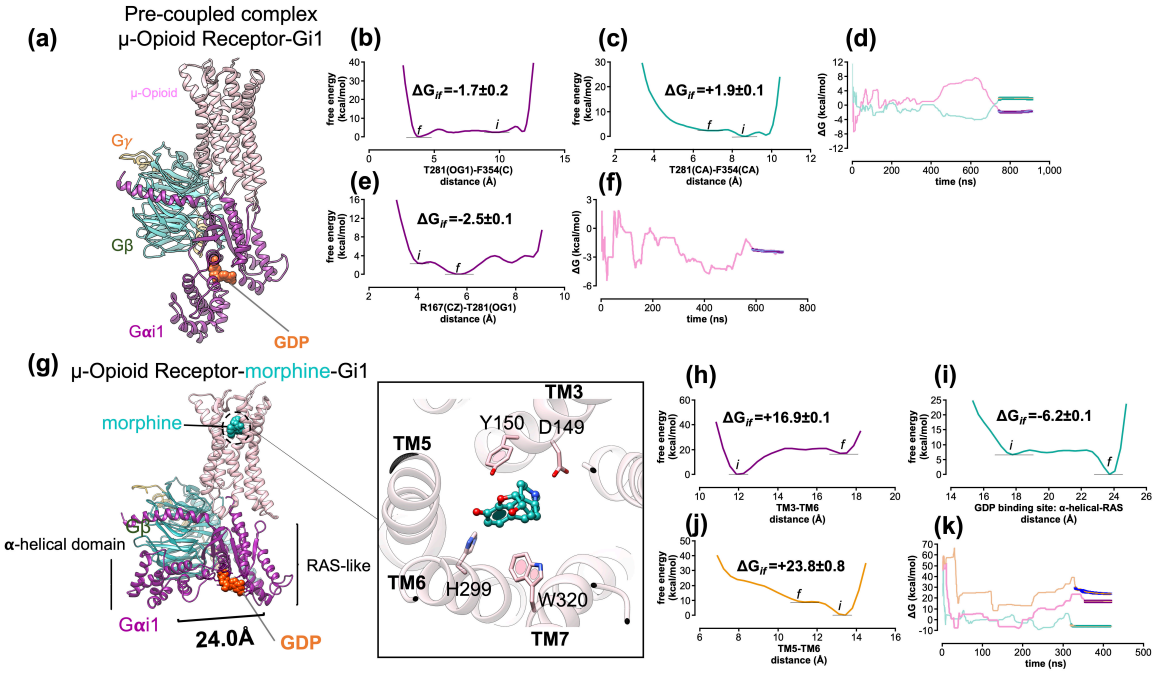

Figure S3. Sequence of the activation process for μ-opioid receptor and Gi1 protein according to the G Protein-First activation mechanism. **(a)** pre-coupled complex formation between μ-opioid receptor – Gi1 protein before ligand binding; agonist binding to the pre-coupled state drives the complex to its activated state by **(g)** opening the Gi1 protein from its GDP binding site. **(b-c)**, **(e)**, & **(h-j)** metaD free energy calculations for the key collective variables. **(d)**, **(f)**, & **(k)** The variation of the free energy difference with time was calculated to monitor the free energy convergence. The weighted averages and the standard deviations (shown by blue, & orange bands in **(d)**, **(f)**, & **(k)**) were calculated for the converged period. Adopted from Figure 5-6 of Mafi et al. (*32*).

A_{2A}-Adenosine Receptor-Gs

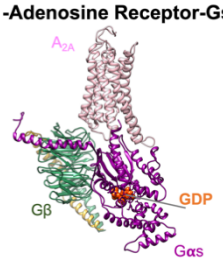

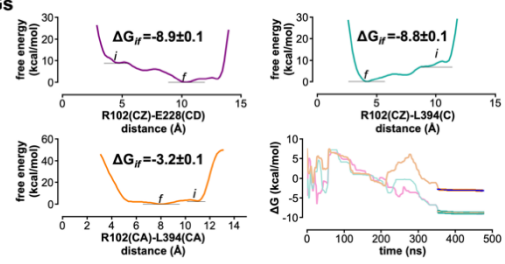

κ-Opioid Receptor-Gi1

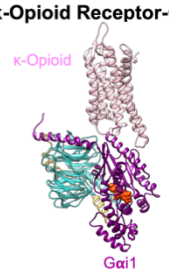

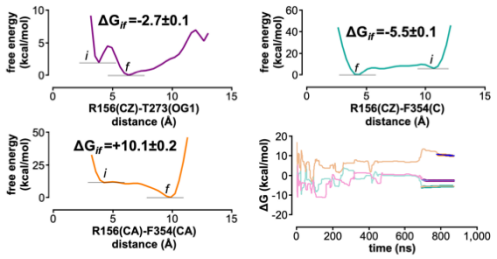

δ-Opioid Receptor-Gi1

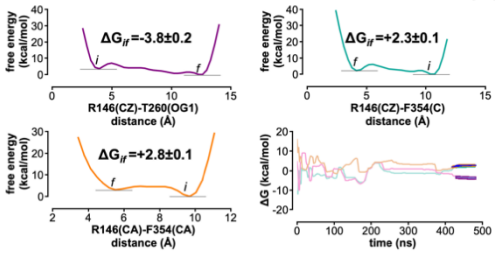

C-C Chemokine Receptor 5-Gi1

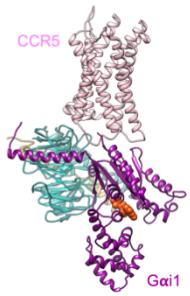

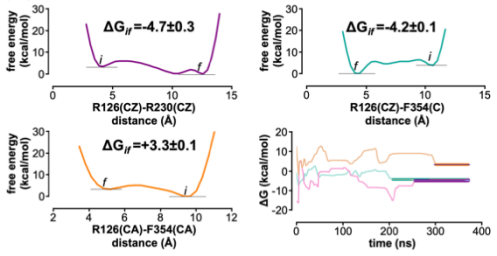

CB1-Cannabinoid Receptor-Gi1

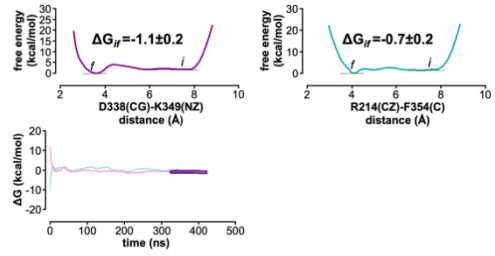

A_1-Adenosine Receptor-Gi2

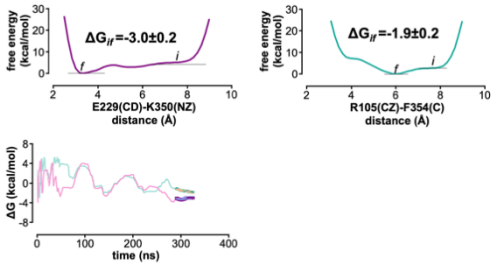

5-HT_{1B}-Serotonin Receptor-Go

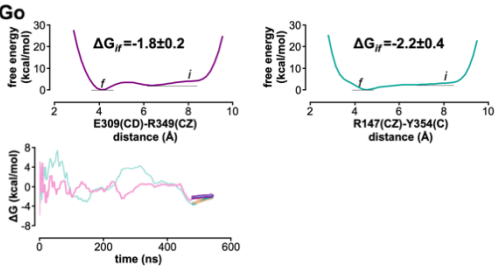

D_2-Dopamine Receptor-Go

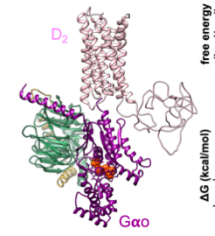

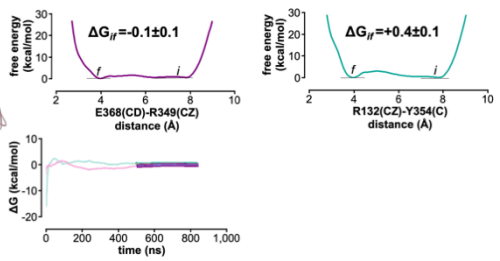

M_1-Muscarinic Receptor-G11

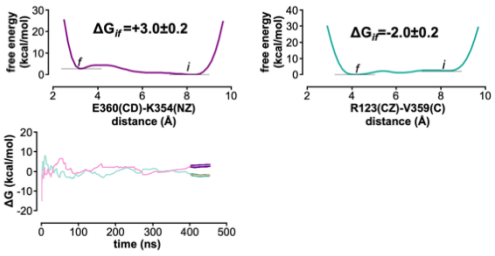

M_3-Muscarinic Receptor-Gq

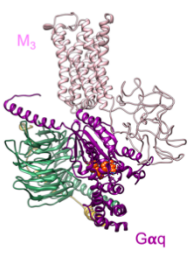

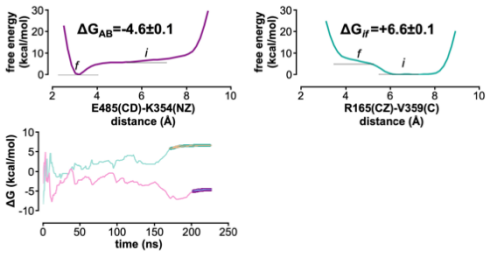

α_{2A}-Adrenergic Receptor-Gq

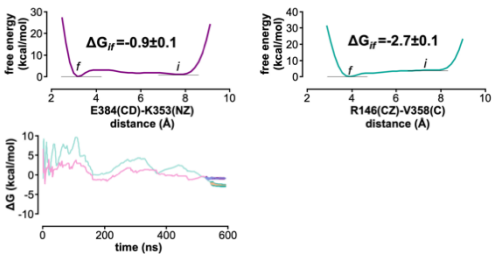

5-HT_{2C}-Serotonin Receptor-Gq

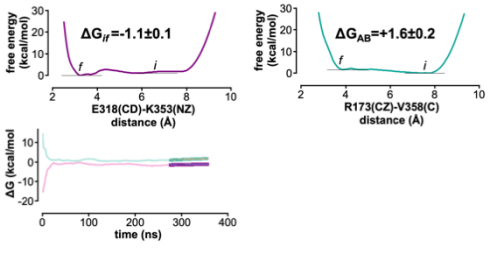

Figure S4. Pre-coupled complex formation between class A GPCRs and their cognate G proteins accompanied with energetics of key variables (as also represented in Table S3) obtained from performing ~7 μs metaD simulations. The weighted averages and the standard deviations (shown by blue, & orange bands) were calculated for the converged period.

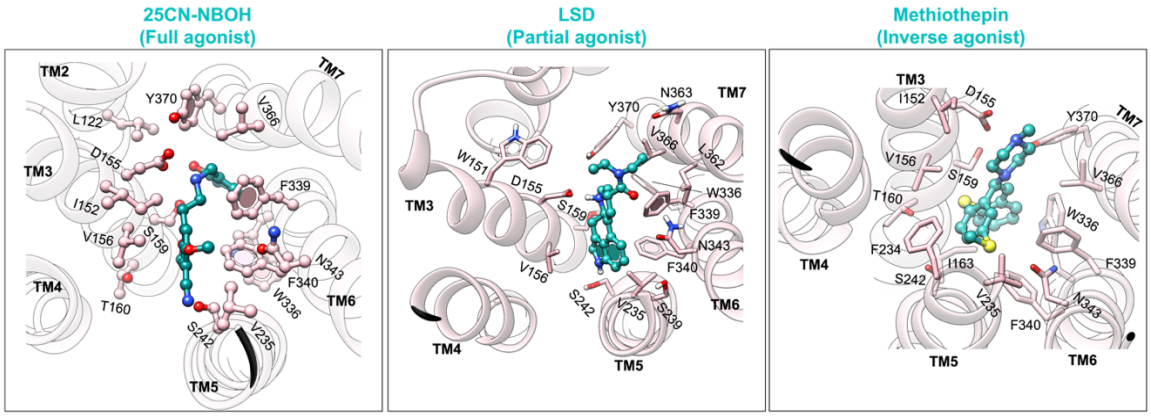

Figure S5. The optimized orthosteric binding pocket of different types of ligands on the pre-coupled 5-HT$_{2A}$-Gq protein.

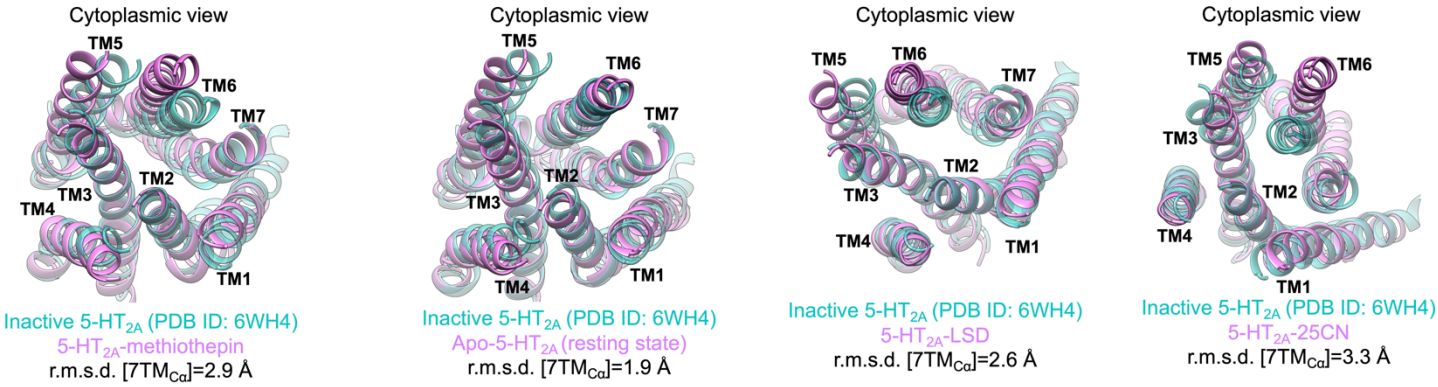

Figure S6. Comparison of the cytoplasmic region of 5-HT$_{2A}$ in the presence of [from left to right]: methiothepin (inverse agonist), apo, LSD (partial agonist), and 25CN-NBOH (full agonist) with the inactive conformation(*1*) of 5-HT$_{2A}$ (PDB ID: 6WH4) resolved by X-ray crystallography.

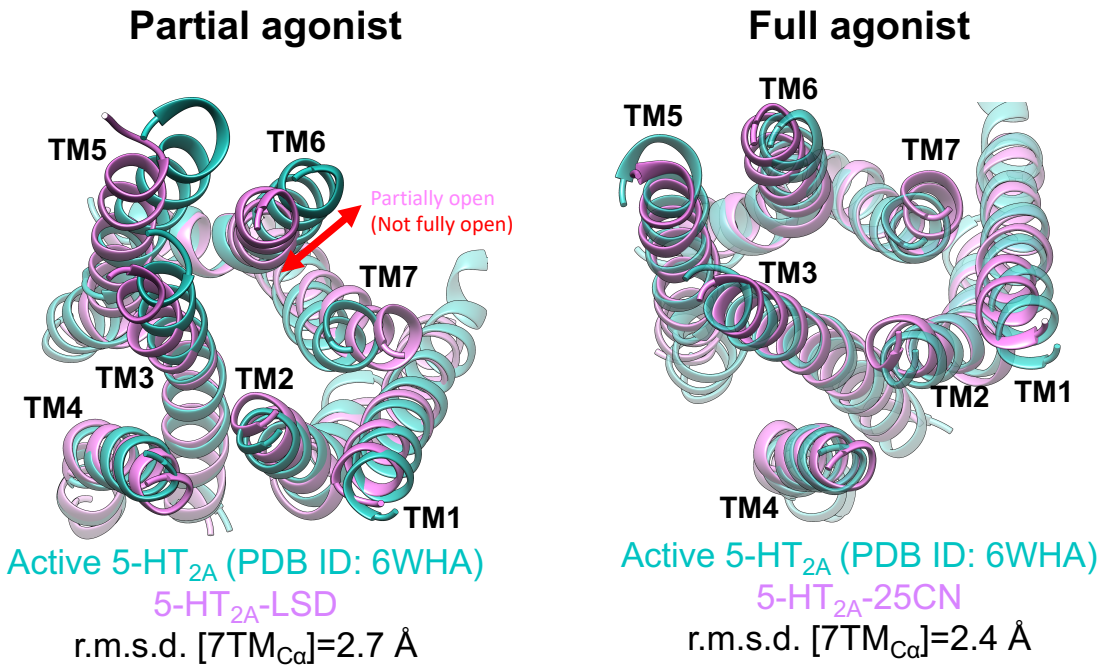

Figure S7. Comparison of the cytoplasmic region of 5-HT$_{2A}$ in its active state in the presence of left: LSD, partial agonist (partially open), and Right: 25CN-NBOH, full agonist (fully open) with the fully activated state(*1*) of 5-HT$_{2A}$ (PDB ID: 6WHA) resolved by cryo-EM.

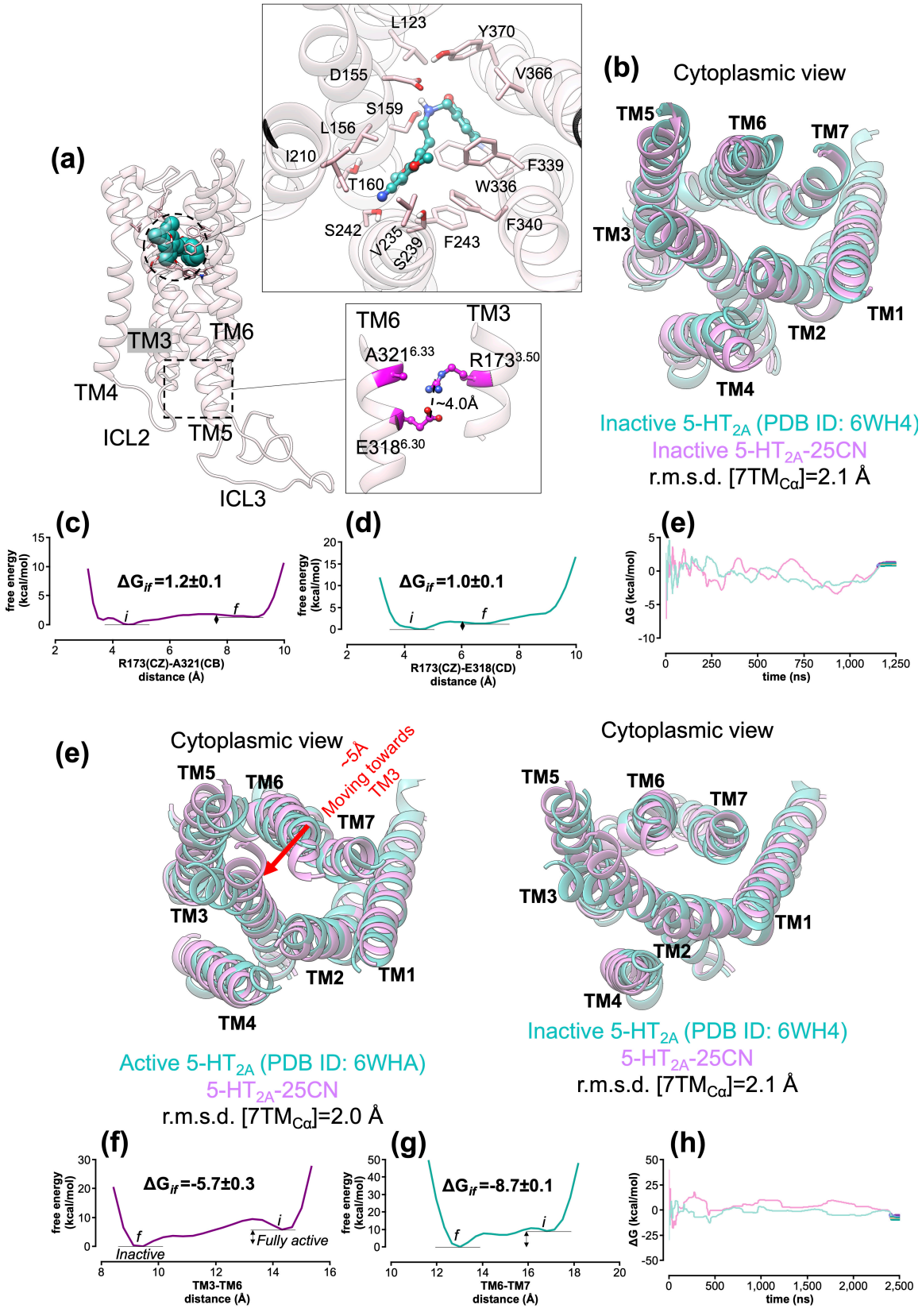
(a)
L123
Y370
D155
V366
S159
L156
I210
F339
T160
W336
S242
F340
V235
S239
F243
TM3
TM6
TM4
ICL2
TM5
ICL3
TM6
TM3
A321 6.33
R173 3.50
~4.0Å
E318 6.30
(b)
Cytoplasmic view
TM5
TM6
TM7
TM3
TM1
TM2
TM4
Inactive 5-HT2A (PDB ID: 6WH4)
Inactive 5-HT2A-25CN
r.m.s.d. [7TMCα]=2.1 Å
(c)
free energy (kcal/mol)
ΔGif=1.2±0.1
i
f
R173(CZ)-A321(CB) distance (Å)
(d)
free energy (kcal/mol)
ΔGif=1.0±0.1
i
f
R173(CZ)-E318(CD) distance (Å)
(e)
ΔG (kcal/mol)
time (ns)
(e)
Cytoplasmic view
~5Å
Moving towards TM3
TM5
TM6
TM7
TM3
TM2
TM1
TM4
Active 5-HT2A (PDB ID: 6WHA)
5-HT2A-25CN
r.m.s.d. [7TMCα]=2.0 Å
Cytoplasmic view
TM5
TM6
TM7
TM3
TM1
TM2
TM4
Inactive 5-HT2A (PDB ID: 6WH4)
5-HT2A-25CN
r.m.s.d. [7TMCα]=2.1 Å
(f)
free energy (kcal/mol)
ΔGif=-5.7±0.3
f
Inactive
i
Fully active
TM3-TM6 distance (Å)
(g)
free energy (kcal/mol)
ΔGif=-8.7±0.1
f
i
TM6-TM7 distance (Å)
(h)
ΔG (kcal/mol)
time (ns)

Figure S8. Full agonist cannot stabilize the active state nor open up the ionic lock in the inactive state conformation of 5-HT_{2A}. (a) Inactive 5-HT_{2A}-bound 25CN-NBOH. **(b)** Comparison of the cytoplasmic region of optimized 5-HT_{2A}-bound 25CN-NBOH with the inactive conformation(*1*) of 5-HT_{2A} (PDB ID: 6WH4) resolved by X-ray crystallography. **(e)** The cytoplasmic region of 5-HT_{2A}-bound 25CN-NBOH derived from the active state conformation(*1*) of 5-HT_{2A} (PDB ID: 6WHA) after eliminating the Gq protein form the complex. Left panel: comparison of optimized 5-HT_{2A}-bound 25CN-NBOH with the active state conformation(*1*) of 5-HT_{2A} (PDB ID: 6WHA); Right panel: comparison of optimized 5-HT_{2A}-bound 25CN-NBOH with the inactive state conformation(*1*) of 5-HT_{2A} (PDB ID: 6WH4), indicating that a full agonist alone cannot stabilize the active state conformation of 5-HT_{2A}. metaD free energy of: **(c-d)** opening the TM3-TM6 coupling (as also represented in Table S5); & (**f-g**) key variables associated with the stability of active state conformation ((as also represented in Table S5). (**h**) & (**e**) The variation of the free energy difference with time was calculated to monitor the free energy convergence. The weighted averages and the standard deviations (shown by blue & orange bands) were calculated for the converged period.

Table S1. MetaD free energy calculations using Charmm36m(*14*) for Gq Protein-First mechanism of activation of 5-HT$_{2A}$ and Gq protein.

Calculation#	System	Size (atoms #, box)	MetaD parameters	Collective Variables (CV)	Upper/Lower walls	Duration
1	Pre-coupled complex 5-HT$_{2A}$-Gq-GDP	POPC #=350 Total #=206K Box=115×115×150Å^3	Every 1ps Height=0.48kcal.mol^{-1} σ=[0.5, 0.5]Å Bias factor=15	CV1=Distance [R173(CZ) V358(C)] CV2=Distance [E318(CD) K353(NZ)]	Upper wall1 ={CV1<9.0 Å, with force constant=12.0 kcal.mol^{-1}Å^{-2}} Upper wall2 ={CV1<9.0 Å, with force constant=12.0 kcal.mol^{-1}Å^{-2}}	~0.4μs
2	Pre-coupled complex 5-HT$_{2A}$-Gq-GDP	POPC #=350 Total #=206K Box=115×115×150Å^3	Every 1ps Height=0.48kcal.mol^{-1} σ=[0.5, 0.5, 0.5]Å Bias factor=15	CV1=Distance [R173(CZ) V358(C)] CV2=Distance [E318(CD) K353(NZ)] CV3=Distance [R173(CZ) E318(CD)]	Upper wall1 ={CV1<9.0 Å, with force constant=12.0 kcal.mol^{-1}Å^{-2}} Upper wall2 ={CV2<9.0 Å, with force constant=12.0 kcal.mol^{-1}Å^{-2}} Upper wall3 ={CV3<9.0 Å, with force constant=12.0 kcal.mol^{-1}Å^{-2}}	~0.6μs
3	Pre-coupled complex 5-HT$_{2A}$-Gαq5 peptide	POPC #=111 Total #=49K Box=66×66×108Å^3	Every 1ps Height=0.48kcal.mol^{-1} σ=[0.5, 0.5, 0.5]Å Bias factor=15	CV1=Distance [R173(CZ) V358(C)] CV2=Distance [E318(CD) K353(NZ)] CV3=Distance [R173(CZ) E318(CD)]	Upper wall1 ={CV1<9.0 Å, with force constant=12.0 kcal.mol^{-1}Å^{-2}} Upper wall2 ={CV2<9.0 Å, with force constant=12.0 kcal.mol^{-1}Å^{-2}} Upper wall3 ={CV3<9.0 Å, with force constant=12.0 kcal.mol^{-1}Å^{-2}}	~1.4μs
4	25CN-NBOH [full agonist]-5-HT$_{2A}$-Gq-GDP complex	POPC #=350 Total #=206K Box=115×115×150Å^3	Every 1ps Height=0.72kcal.mol^{-1} σ=[1.0, 1.0, 1.0]Å Bias factor=25	CV1=Distance [AH domain (*center of mass of Cα for the residues 154-161 and 175-182*) --- Ras-like domain (*center of mass of Cα for the residues 51-62*)] CV2=Distance [TM3 (*the center of mass of Cα for residues 168-178*) --- TM6 (*the center of mass of Cα for residues 318-328*)] CV3=Distance [TM6 (*the center of mass of Cα for residues 318-328*) --- TM7 (*the center of mass of Cα for residues 372-382*)]	Upper wall1 ={CV1<23.0 Å, with force constant=24.0 kcal.mol^{-1}Å^{-2}} Lower wall1 ={CV1>16.0 Å, with force constant=24.0 kcal.mol^{-1}Å^{-2}} Upper wall2 ={CV2<15.5 Å, with force constant=24.0 kcal.mol^{-1}Å^{-2}} Lower wall2 ={CV2>13.0 Å, with force constant=24.0 kcal.mol^{-1}Å^{-2}}	~0.2μs

					Upper wall3 ={CV3<17.0 Å, with force constant=24.0 kcal.mol^{-1}Å^{-2}} Lower wall3 ={CV3>13.0 Å, with force constant=24.0 kcal.mol^{-1}Å^{-2}} Upper wall4 ={Distance [TM6 (*the center of mass of Cα for residues 318-328*) --- TM5 (*the center of mass of Cα for residues 253-263*)]<14.0 Å, with force constant=24.0 kcal.mol^{-1}Å^{-2}} Upper wall5 ={Distance [K320 (CB) --- V358 (C)]<8.0 Å, with force constant=2.4 kcal.mol^{-1}Å^{-2}}	
5	LSD [partial agonist]-5-HT$_{2A}$-Gq-GDP complex	POPC #=350 Total #=206K Box=115×115×150Å^3	Every 1ps Height=0.72kcal.mol^{-1} σ=[1.0, 1.0, 1.0]Å Bias factor=25	CV1=Distance [AH domain (*center of mass of Cα for the residues 154-161 and 175-182*) --- Ras-like domain (*center of mass of Cα for the residues 51-62*)] CV2=Distance [TM3 (*the center of mass of Cα for residues 168-178*) --- TM6 (*the center of mass of Cα for residues 318-328*)] CV3=Distance [TM6 (*the center of mass of Cα for residues 318-328*) --- TM7 (*the center of mass of Cα for residues 372-382*)]	Same as calculation # 4	~0.2μs
6	Methiothepin [inverse agonist]-5-HT$_{2A}$-Gq-GDP complex	POPC #=350 Total #=206K Box=115×115×150Å^3	Every 1ps Height=0.72kcal.mol^{-1} σ=[1.0, 1.0, 1.0]Å Bias factor=25	CV1=Distance [AH domain (*center of mass of Cα for the residues 154-161 and 175-182*) --- Ras-like domain (*center of mass of Cα for the residues 51-62*)] CV2=Distance [TM3 (*the center of mass of Cα for residues 168-178*) --- TM6 (*the center of mass of Cα for residues 318-328*)] CV3=Distance [TM6 (*the center of mass of Cα for residues 318-328*) --- TM7 (*the center of mass of Cα for residues 372-382*)]	Same as calculation # 4	~0.2μs
7	apo-5-HT$_{2A}$-Gq-GDP complex	POPC #=350	Every 1ps Height=0.72kcal.mol^{-1} σ=[1.0, 1.0, 1.0]Å	CV1=Distance [AH domain (*center of mass of Cα for the residues*	Same as calculation # 4	~0.3μs

		Total #=206K Box=115×115×150Å^3	Bias factor=25	*154-161 and 175-182*) --- Ras-like domain (*center of mass of Cα for the residues 51-62*)] CV2=Distance [TM3 (*the center of mass of Cα for residues 168-178*) --- TM6 (*the center of mass of Cα for residues 318-328*)] CV3=Distance [TM6 (*the center of mass of Cα for residues 318-328*) --- TM7 (*the center of mass of Cα for residues 372-382*)]		

Table S2. MetaD free energy calculations using AMBER14(*15*) for Gs Protein-First mechanism of activation of β_2AR and Gs protein.

#	System	Size (atoms #, box)	MetaD parameters	Collective Variables (CV)	Upper/Lower walls	Duration
1	Inactive β_2AR-T4L	POPC #=277 Total #=110K Box=103×103×102Å^3	Every 1ps Height=0.24kcal.mol^{-1} σ=[0.5, 0.5]Å Bias factor=12 # of Walker=1	CV1=Distance [R131$^{3.50}$(CG)-L272$^{6.34}$(CD2)] CV2=Distance [R131$^{3.50}$(CZ)-E268$^{6.30}$(CD)]	Upper wall1 ={CV1<11.0 Å, with force constant=24.0 kcal.mol^{-1}Å^{-2}} Upper wall2 ={CV1<9.0 Å, with force constant=24.0 kcal.mol^{-1}Å^{-2}}	~0.6μs
2	Inactive β_2AR-T4L	POPC #=277 Total #=110K Box=103×103×102Å^3	Every 1ps Height=0.24kcal.mol^{-1} σ=[0.5, 0.5]Å Bias factor=12	CV1=Distance [R131$^{3.50}$(CG)-L272$^{6.34}$(CD2)] CV2=Distance [R131$^{3.50}$(CZ)-E268$^{6.30}$(CD)]	Upper wall1 ={CV1<11.0 Å, with force constant=24.0 kcal.mol^{-1}Å^{-2}} Upper wall2 ={CV1<9.0 Å, with force constant=24.0 kcal.mol^{-1}Å^{-2}}	~1.6μs
3	Pre-coupled complex β_2AR-Gs-GDP	POPC #=277 Total #=167K Box=103×103×156Å^3	Every 1ps Height=0.48kcal.mol^{-1} σ=[0.5, 0.5, 0.5]Å Bias factor=15	CV1=Distance [R131$^{3.50}$(CZ)-E392(CD)] CV2=Distance [E268$^{6.30}$(CD)-R389(CZ)] CV3=Distance [E237$^{5.66}$(CD)-R385(CZ)]	Upper wall1 ={CV1<12.0 Å, with force constant=24.0 kcal.mol^{-1}Å^{-2}} Upper wall2 ={CV2<9.0 Å, with force constant=24.0 kcal.mol^{-1}Å^{-2}} Upper wall3 ={CV3<9.0 Å, with force constant=24.0 kcal.mol^{-1}Å^{-2}}	~0.8μs

Table S3. MetaD free energy calculations using ChARMM36m(*14*) for G Protein-First mechanism of activation of class A GPCRs and their cognate G proteins.

#	system	Inactive template (PDB ID)	Active template (PDB ID)	Size (atoms #, box)	MetaD parameters	Collective Variables (CV)	Upper wall (UW)/Lower wall (LW)	Duration
1	**A_{2A}-Adenosine-Gs**	3EML(*33*)	3SN6(*34*)	POPC #=277 Total #=~167K Box=100×100×165Å^3 # Walkers_MPI=1	Every 1ps Hight=0.48 kcal.mol^{-1} σ=[0.5, 0.5, 0.5]Å Bias factor=15	CV1=Distance [R126$^{3.50}$(CZ)-L394(C)] CV2=Distance [R126$^{3.50}$(CZ)-E228$^{3.50}$(CD)] CV3=Distance [R126$^{3.50}$(CA)-L394(CA)]	UW1 ={CV1<11.0 Å, with force constant=24.0 kcal.mol^{-1}Å^{-2}} UW2 ={CV1<13.0 Å, with force constant=24.0 kcal.mol^{-1}Å^{-2}} UW3 ={CV3<11.0 Å, with force constant=24.0 kcal.mol^{-1}Å^{-2}}	~0.5μs
2	**κ-Opioid-Gi1**	4DJH(*35*)	6DDF(*36*)	POPC #=277 Total #=~167K Box=102×102×156Å^3 # Walkers_MPI=1	Every 1ps Height=0.48 kcal.mol^{-1} σ=[1.0, 1.0, 1.0]Å Bias factor=25	CV1=Distance [R156$^{3.50}$(CZ)-F354(C)] CV2=Distance [R156$^{3.50}$(CA)-F354(CA)] CV3=Distance [R156$^{3.50}$(CZ)-T273$^{6.34}$(OG1)]	UW1 ={CV1<11.0 Å, with force constant=24.0 kcal.mol^{-1}Å^{-2}} UW2 ={CV1<10.0 Å, with force constant=24.0 kcal.mol^{-1}Å^{-2}} UW3 ={CV3<13.0 Å, with force constant=24.0 kcal.mol^{-1}Å^{-2}}	~0.9μs
3	**δ-Opioid-Gi1**	4N6H(*37*)	6DDF(*36*)	POPC #=277 Total #=~167K Box=102×102×156Å^3 # Walkers_MPI=1	Every 1ps Height=0.48 kcal.mol^{-1} σ=[1.0, 1.0, 1.0]Å Bias factor=15	CV1=Distance [R146$^{3.50}$(CZ)-F354(C)] CV2=Distance [R146$^{3.50}$(CA)-F354(CA)] CV3=Distance [R146$^{3.50}$(CZ)-T260$^{6.34}$(OG1)]	UW1 ={CV1<11.0 Å, with force constant=24.0 kcal.mol^{-1}Å^{-2}} UW2 ={CV1<13.0 Å, with force constant=24.0 kcal.mol^{-1}Å^{-2}} UW3 ={CV3<10.0 Å, with force constant=24.0 kcal.mol^{-1}Å^{-2}}	~0.5μs
4	**C-C-Chemokine 5-Gi1**	5UIW(*38*)	6DDF(*36*)	POPC #=277 Total #=~167K Box=102×102×156Å^3 # Walkers_MPI=1	Every 1ps Height=0.48 kcal.mol^{-1} σ=[1.0, 1.0, 1.0]Å Bias factor=15	CV1=Distance [R126$^{3.50}$(CZ)-F354(C)] CV2=Distance [R126$^{3.50}$(CA)-F354(CA)] CV3=Distance [R126$^{3.50}$(CZ)-R230$^{6.30}$(CZ)]	UW1 ={CV1<11.0 Å, with force constant=24.0 kcal.mol^{-1}Å^{-2}} UW2 ={CV1<10.0 Å, with force constant=24.0 kcal.mol^{-1}Å^{-2}} UW3 ={CV3<13.0 Å, with force constant=24.0 kcal.mol^{-1}Å^{-2}}	~0.4μs
5	**CB1-Cannabinoid - Gi1**	5TGZ(*39*)	6N4B(*40*)	POPC #=361 Total #=~230K Box=113×113×154Å^3 # Walkers_MPI=10	Every 1ps Height=0.48 kcal.mol^{-1} σ=[0.2, 0.2]Å Bias factor=15	CV1=Distance [R214$^{3.50}$(CZ)-F354(C)] CV2=Distance [D338$^{6.30}$(CG)-K349(NZ)]	UW1 ={CV1<7.8 Å, with force constant=20.0 kcal.mol^{-1}Å^{-2}} UW2 ={CV2<7.8 Å, with force constant=20.0 kcal.mol^{-1}Å^{-2}}	~0.4μs

6	**A_1-Adenosine-Gi2**	5UEN(*41*)	6D9H(*42*)	POPC #=257 Total #=~152K Box=101×101×161Å^3 # Walkers_MPI=1	Every 1ps Height=0.48 kcal.mol^{-1} σ=[0.5, 0.5]Å Bias factor=15	CV1=Distance [R214$^{3.50}$(CZ)-F355(C)] CV2=Distance [E229$^{6.30}$(CG)-K350(NZ)]	UW1 ={CV1<8.0 Å, with force constant=20.0 kcal.mol^{-1}Å^{-2}} UW2 ={CV2<8.0 Å, with force constant=20.0 kcal.mol^{-1}Å^{-2}}	~0.3μs
7	**5-HT_{1B}-Serotonin-Go**	5V54(*43*)	6G79(*44*)	POPC #=379 Total #=~214K Box=115×115×156Å^3 # Walkers_MPI=1	Every 1ps Height=0.48 kcal.mol^{-1} σ=[0.5, 0.5]Å Bias factor=15	CV1=Distance [R147$^{3.50}$(CZ)-Y354(C)] CV2=Distance [E309$^{6.30}$(CG)-R349(CZ)]	UW1 ={CV1<8.5 Å, with force constant=20.0 kcal.mol^{-1}Å^{-2}} UW2 ={CV2<8.5 Å, with force constant=20.0 kcal.mol^{-1}Å^{-2}}	~0.6μs
8	**D_2-Dopamine-Go**	6LUQ(*45*)	6VMS(*46*)	POPC #=291 Total #=~164K Box=104×104×148Å^3 # Walkers_MPI=32	Every 1ps Height=0.48 kcal.mol^{-1} σ=[0.2, 0.2]Å Bias factor=15	CV1=Distance [R132$^{3.50}$(CZ)-Y354(C)] CV2=Distance [E368$^{6.30}$(CG)-R349(CZ)]	UW1 ={CV1<8.5 Å, with force constant=20.0 kcal.mol^{-1}Å^{-2}} UW2 ={CV2<8.5 Å, with force constant=20.0 kcal.mol^{-1}Å^{-2}}	~0.9μs
9	**M_1-Muscarinic-G11**	6WJC(*47*)	6OIJ(*48*)	POPC #=269 Total #=~155K Box=98×98×157Å^3 # Walkers_MPI=1	Every 1ps Height=0.48 kcal.mol^{-1} σ=[0.5, 0.5]Å Bias factor=15	CV1=Distance [R123$^{3.50}$(CZ)-V359(C)] CV2=Distance [E360$^{6.30}$(CG)-K354(NZ)]	UW1 ={CV1<8.5 Å, with force constant=20.0 kcal.mol^{-1}Å^{-2}} UW2 ={CV2<8.5 Å, with force constant=20.0 kcal.mol^{-1}Å^{-2}}	~0.5μs
10	**M_3-Muscarinic-Gq**	5ZHP(*49*)	6OIJ(*48*)	POPC #=388 Total #=~203K Box=117×117×144Å^3 # Walkers_MPI=1	Every 1ps Height=0.48 kcal.mol^{-1} σ=[0.5, 0.5]Å Bias factor=15	CV1=Distance [R165$^{3.50}$(CZ)-V359(C)] CV2=Distance [E485$^{6.30}$(CG)-K354(NZ)]	UW1 ={CV1<8.0 Å, with force constant=20.0 kcal.mol^{-1}Å^{-2}} UW2 ={CV2<8.0 Å, with force constant=20.0 kcal.mol^{-1}Å^{-2}}	~0.3μs
11	**α_{2A}-Adrenergic-Gq**	6KUX	6K41(*50*)	POPC #=312 Total #=~177K Box=110×110×158Å^3 # Walkers_MPI=1	Every 1ps Height=0.48 kcal.mol^{-1} σ=[0.5, 0.5]Å Bias factor=15	CV1=Distance [R146$^{3.50}$(CZ)-V358(C)] CV2=Distance [E384$^{6.30}$(CG)-K353(NZ)]	UW1 ={CV1<8.0 Å, with force constant=20.0 kcal.mol^{-1}Å^{-2}} UW2 ={CV2<8.0 Å, with force constant=20.0 kcal.mol^{-1}Å^{-2}}	~0.6μs
12	**5-HT_{2C}-Serotonin-Gq**	6BQH(*51*)	6WHA[3]	POPC #=350 Total #=~206K Box=115×115×155Å^3 # Walkers_MPI=32	Every 1ps Height=0.48 kcal.mol^{-1} σ=[0.2, 0.2]Å Bias factor=15	CV1=Distance [R173$^{3.50}$(CZ)-V358(C)] CV2=Distance [E318$^{6.30}$(CG)-K353(NZ)]	UW1 ={CV1<7.8 Å, with force constant=20.0 kcal.mol^{-1}Å^{-2}} UW2 ={CV2<7.8 Å, with force constant=20.0 kcal.mol^{-1}Å^{-2}}	~0.4μs

Table S4. MetaD free energy calculations using ChARMM36m(*14*) for agonist activation of Protein-pre-coupled A_{2A} receptor-Gs protein-GDP complex.

#	System	Size (atoms #, box)	MetaD parameters	Collective Variables (CV)	Upper/Lower walls	Duration
1	**A_{2A}-NECA-Gs-GDP**	POPC #=280 Cholesterol #=65 Total #=~175K Box=110×110×156 $Å^3$ # Walkers_MPI=1	Every 1ps Height=0.72kcal. mol^{-1} σ=[1.0, 1.0]Å Bias factor=25	CV1=Distance [AH domain (*center of mass of Cα for the residues 69-204*) --- Ras-like domain (*center of mass of Cα for the residues 49-65, 223-241, 294-303, and 369-374*)] CV2=Distance [TM3 (*the center of mass of Cα for residues 97-107*) --- TM6 (*the center of mass of Cα for residues 223-233*)]	UW1 ={CV1<19.0 Å, with force constant=60.0 kcal.$mol^{-1}Å^{-2}$} LW1 ={CV1>12.0 Å, with force constant=60.0 kcal.$mol^{-1}Å^{-2}$} UW2 ={CV1<31.6 Å, with force constant=60.0 kcal.$mol^{-1}Å^{-2}$} LW2 ={CV1>21.6 Å, with force constant=60.0 kcal.$mol^{-1}Å^{-2}$}	~1.2μs

Table S5. MetaD free energy calculations for Ligand-First mechanism of activation.

#	system	Initial state	Size (atoms #, box)	MetaD parameters	Collective Variables (CV)	Upper wall (UW)/Lower wall (LW)	Force field	Duration
1	25CN-NBOH-5-HT_{2A}	Inactive	POPC #=111 Total #=49K Box=66×66×108Å^3	Every 1ps Height=0.48 kcal.mol^{-1} σ=[0.5, 0.5]Å Bias factor=15	CV1=Distance [R173$^{3.50}$(CZ)-E318$^{6.30}$(CD)] CV2=Distance [R173$^{3.50}$(CZ)-A321$^{6.33}$(CB)]	UW1 ={CV1<9.0 Å, with force constant=12.0 kcal.mol^{-1}Å^{-2}} UW2 ={CV2<9.0 Å, with force constant=12.0 kcal.mol^{-1}Å^{-2}}	ChARMM36m(*14*)	~1.3μs
2	25CN-NBOH-5-HT_{2A}	Active	POPC #=132 Total #=49K Box=75×75×92Å^3	Every 1ps Height=0.72 kcal.mol^{-1} σ=[1.0, 1.0]Å Bias factor=25	CV1=Distance [TM3 (*the center of mass of Cα for residues 168-178*) --- TM6 (*the center of mass of Cα for residues 318-328*)] CV1=Distance [TM6 (*the center of mass of Cα for residues 318-328*) --- TM7 (*the center of mass of Cα for residues 372-382*)]	UW1 ={CV1<14.5 Å, with force constant=24.0 kcal.mol^{-1}Å^{-2}} LW1 ={CV1>9.0 Å, with force constant=24.0 kcal.mol^{-1}Å^{-2}} UW2 ={CV2<17.0 Å, with force constant=24.0 kcal.mol^{-1}Å^{-2}} LW2 ={CV2>13.0 Å, with force constant=24.0 kcal.mol^{-1}Å^{-2}}	ChARMM36m(*14*)	~2.5μs

SI References

1. K. Kim, T. Che, O. Panova, J. F. DiBerto, J. Lyu, B. E. Krumm, D. Wacker, M. J. Robertson, A. B. Seven, D. E. Nichols, Structure of a hallucinogen-activated gq-coupled 5-ht2a serotonin receptor. *Cell*. **182**, 1574–1588 (2020).

2. N. Eswar, D. Eramian, B. Webb, M.-Y. Shen, A. Sali, in *Structural proteomics* (Springer, 2008), pp. 145–159.

3. M. A. Wall, D. E. Coleman, E. Lee, J. A. Iñiguez-Lluhi, B. A. Posner, A. G. Gilman, S. R. Sprang, The structure of the G protein heterotrimer Giα1β1γ2. *Cell*. **83**, 1047–1058 (1995).

4. D. G. Lambright, J. Sondek, A. Bohm, N. P. Skiba, H. E. Hamm, P. B. Sigler, The 2.0 \AA crystal structure of a heterotrimeric G protein. *Nature*. **379**, 311–319 (1996).

5. S. B. Needleman, C. D. Wunsch, A general method applicable to the search for similarities in the amino acid sequence of two proteins. *J. Mol. Biol.* **48**, 443–453 (1970).

6. E. F. Pettersen, T. D. Goddard, C. C. Huang, G. S. Couch, D. M. Greenblatt, E. C. Meng, T. E. Ferrin, UCSF Chimera—a visualization system for exploratory research and analysis. *J. Comput. Chem.* **25**, 1605–1612 (2004).

7. E. L. Wu, X. Cheng, S. Jo, H. Rui, K. C. Song, E. M. Dávila-Contreras, Y. Qi, J. Lee, V. Monje-Galvan, R. M. Venable, *CHARMM-GUI membrane builder toward realistic biological membrane simulations* (Wiley Online Library, 2014).

8. V. Cherezov, D. M. Rosenbaum, M. A. Hanson, S. G. Rasmussen, F. S. Thian, T. S. Kobilka, H.-J. Choi, P. Kuhn, W. I. Weis, B. K. Kobilka, High-resolution crystal structure of an engineered human β2-adrenergic G protein–coupled receptor. *science*. **318**, 1258–1265 (2007).

9. A. Barducci, G. Bussi, M. Parrinello, Well-tempered metadynamics: a smoothly converging and tunable free-energy method. *Phys. Rev. Lett.* **100**, 020603 (2008).

10. X. Liu, X. Xu, D. Hilger, P. Aschauer, J. K. Tiemann, Y. Du, H. Liu, K. Hirata, X. Sun, R. Guixà-González, Structural insights into the process of GPCR-G protein complex formation. *Cell*. **177**, 1243–1251 (2019).

11. Q. Hu, K. M. Shokat, Disease-causing mutations in the G protein Gαs subvert the roles of GDP and GTP. *Cell*. **173**, 1254–1264 (2018).

12. S. G. Rasmussen, B. T. DeVree, Y. Zou, A. C. Kruse, K. Y. Chung, T. S. Kobilka, F. S. Thian, P. S. Chae, E. Pardon, D. Calinski, Crystal structure of the β 2 adrenergic receptor–Gs protein complex. *Nature*. **477**, 549–555 (2011).

13. N. Guex, M. C. Peitsch, SWISS-MODEL and the Swiss-Pdb Viewer: an environment for comparative protein modeling. *electrophoresis*. **18**, 2714–2723 (1997).

14. J. Huang, S. Rauscher, G. Nawrocki, T. Ran, M. Feig, B. L. de Groot, H. Grubmüller, A. D. MacKerell Jr, CHARMM36m: an improved force field for folded and intrinsically disordered proteins. *Nat. Methods*. **14**, 71 (2017).

15. C. J. Dickson, B. D. Madej, \AAge A. Skjevik, R. M. Betz, K. Teigen, I. R. Gould, R. C. Walker, Lipid14: the amber lipid force field. *J. Chem. Theory Comput.* **10**, 865–879 (2014).

16. J. Wang, R. M. Wolf, J. W. Caldwell, P. A. Kollman, D. A. Case, Development and testing of a general amber force field. *J. Comput. Chem.* **25**, 1157–1174 (2004).

17. A. W. S. da Silva, W. F. Vranken, ACPYPE-Antechamber python parser interface. *BMC Res. Notes*. **5**, 367 (2012).

18. J. Wang, W. Wang, P. A. Kollman, D. A. Case, Automatic atom type and bond type perception in molecular mechanical calculations. *J. Mol. Graph. Model.* **25**, 247–260 (2006).

19. A. Jakalian, D. B. Jack, C. I. Bayly, Fast, efficient generation of high-quality atomic charges. AM1-BCC model: II. Parameterization and validation. *J. Comput. Chem.* **23**, 1623–1641 (2002).

20. K. Lindorff-Larsen, S. Piana, K. Palmo, P. Maragakis, J. L. Klepeis, R. O. Dror, D. E. Shaw, Improved side-chain torsion potentials for the Amber ff99SB protein force field. *Proteins Struct. Funct. Bioinforma.* **78**, 1950–1958 (2010).

21. K. L. Meagher, L. T. Redman, H. A. Carlson, Development of polyphosphate parameters for use with the AMBER force field. *J. Comput. Chem.* **24**, 1016–1025 (2003).

22. W. L. Jorgensen, J. Chandrasekhar, J. D. Madura, R. W. Impey, M. L. Klein, Comparison of simple potential functions for simulating liquid water. *J. Chem. Phys.* **79**, 926–935 (1983).

23. K. Vanommeslaeghe, E. Hatcher, C. Acharya, S. Kundu, S. Zhong, J. Shim, E. Darian, O. Guvench, P. Lopes, I. Vorobyov, CHARMM general force field: A force field for drug-like molecules compatible with the CHARMM all-atom additive biological force fields. *J. Comput. Chem.* **31**, 671–690 (2010).

24. K. Vanommeslaeghe, A. D. MacKerell Jr, Automation of the CHARMM General Force Field (CGenFF) I: bond perception and atom typing. *J. Chem. Inf. Model.* **52**, 3144–3154 (2012).

25. G. Bussi, D. Donadio, M. Parrinello, Canonical sampling through velocity rescaling. *J. Chem. Phys.* **126**, 014101 (2007).

26. M. Parrinello, A. Rahman, Polymorphic transitions in single crystals: A new molecular dynamics method. *J. Appl. Phys.* **52**, 7182–7190 (1981).

27. U. Essmann, L. Perera, M. L. Berkowitz, T. Darden, H. Lee, L. G. Pedersen, A smooth particle mesh Ewald method. *J. Chem. Phys.* **103**, 8577–8593 (1995).

28. S. Miyamoto, P. A. Kollman, Settle: An analytical version of the SHAKE and RATTLE algorithm for rigid water models. *J. Comput. Chem.* **13**, 952–962 (1992).

29. B. Hess, P-LINCS: A parallel linear constraint solver for molecular simulation. *J. Chem. Theory Comput.* **4**, 116–122 (2008).

30. M. J. Abraham, T. Murtola, R. Schulz, S. Páll, J. C. Smith, B. Hess, E. Lindahl, GROMACS: High performance molecular simulations through multi-level parallelism from laptops to supercomputers. *SoftwareX*. **1**, 19–25 (2015).

31. G. A. Tribello, M. Bonomi, D. Branduardi, C. Camilloni, G. Bussi, PLUMED 2: New feathers for an old bird. *Comput. Phys. Commun.* **185**, 604–613 (2014).

32. A. Mafi, S.-K. Kim, W. A. Goddard, The G protein-first activation mechanism of opioid receptors by Gi protein and agonists. *QRB Discov.* **2** (2021).

33. V.-P. Jaakola, M. T. Griffith, M. A. Hanson, V. Cherezov, E. Y. Chien, J. R. Lane, A. P. Ijzerman, R. C. Stevens, The 2.6 angstrom crystal structure of a human A2A adenosine receptor bound to an antagonist. *Science*. **322**, 1211–1217 (2008).

34. S. G. Rasmussen, B. T. DeVree, Y. Zou, A. C. Kruse, K. Y. Chung, T. S. Kobilka, F. S. Thian, P. S. Chae, E. Pardon, D. Calinski, Crystal structure of the β 2 adrenergic receptor–Gs protein complex. *Nature*. **477**, 549 (2011).

35. H. Wu, D. Wacker, M. Mileni, V. Katritch, G. W. Han, E. Vardy, W. Liu, A. A. Thompson, X.-P. Huang, F. I. Carroll, Structure of the human κ-opioid receptor in complex with JDTic. *Nature*. **485**, 327–332 (2012).

36. A. Koehl, H. Hu, S. Maeda, Y. Zhang, Q. Qu, J. M. Paggi, N. R. Latorraca, D. Hilger, R. Dawson, H. Matile, Structure of the μ-opioid receptor–G i protein complex. *Nature*. **558**, 547–552 (2018).

37. G. Fenalti, P. M. Giguere, V. Katritch, X.-P. Huang, A. A. Thompson, V. Cherezov, B. L. Roth, R. C. Stevens, Molecular control of δ-opioid receptor signalling. *Nature*. **506**, 191–196 (2014).

38. Y. Zheng, G. W. Han, R. Abagyan, B. Wu, R. C. Stevens, V. Cherezov, I. Kufareva, T. M. Handel, Structure of CC chemokine receptor 5 with a potent chemokine antagonist reveals mechanisms of chemokine recognition and molecular mimicry by HIV. *Immunity*. **46**, 1005–1017 (2017).

39. T. Hua, K. Vemuri, M. Pu, L. Qu, G. W. Han, Y. Wu, S. Zhao, W. Shui, S. Li, A. Korde, Crystal structure of the human cannabinoid receptor CB1. *Cell*. **167**, 750–762 (2016).

40. K. K. Kumar, M. Shalev-Benami, M. J. Robertson, H. Hu, S. D. Banister, S. A. Hollingsworth, N. R. Latorraca, H. E. Kato, D. Hilger, S. Maeda, Structure of a signaling cannabinoid receptor 1-G protein complex. *Cell*. **176**, 448–458 (2019).

41. A. Glukhova, D. M. Thal, A. T. Nguyen, E. A. Vecchio, M. Jörg, P. J. Scammells, L. T. May, P. M. Sexton, A. Christopoulos, Structure of the adenosine A1 receptor reveals the basis for subtype selectivity. *Cell*. **168**, 867–877 (2017).

42. C. J. Draper-Joyce, M. Khoshouei, D. M. Thal, Y.-L. Liang, A. T. Nguyen, S. G. Furness, H. Venugopal, J.-A. Baltos, J. M. Plitzko, R. Danev, Structure of the adenosine-bound human adenosine A 1 receptor–G i complex. *Nature*. **558**, 559–563 (2018).

43. W. Yin, X. E. Zhou, D. Yang, P. W. de Waal, M. Wang, A. Dai, X. Cai, C.-Y. Huang, P. Liu, X. Wang, Crystal structure of the human 5-HT 1B serotonin receptor bound to an inverse agonist. *Cell Discov.* **4**, 1–13 (2018).

44. J. Garcia-Nafria, R. Nehme, P. C. Edwards, C. G. Tate, Cryo-EM structure of the serotonin 5-HT 1B receptor coupled to heterotrimeric G o. *Nature*. **558**, 620–623 (2018).

45. L. Fan, L. Tan, Z. Chen, J. Qi, F. Nie, Z. Luo, J. Cheng, S. Wang, Haloperidol bound D 2 dopamine receptor structure inspired the discovery of subtype selective ligands. *Nat. Commun.* **11**, 1–11 (2020).

46. J. Yin, K.-Y. M. Chen, M. J. Clark, M. Hijazi, P. Kumari, X. Bai, R. K. Sunahara, P. Barth, D. M. Rosenbaum, Structure of a D2 dopamine receptor–G-protein complex in a lipid membrane. *Nature*. **584**, 125–129 (2020).

47. S. Maeda, J. Xu, F. M. N. Kadji, M. J. Clark, J. Zhao, N. Tsutsumi, J. Aoki, R. K. Sunahara, A. Inoue, K. C. Garcia, Structure and selectivity engineering of the M1 muscarinic receptor toxin complex. *Science*. **369**, 161–167 (2020).

48. S. Maeda, Q. Qu, M. J. Robertson, G. Skiniotis, B. K. Kobilka, Structures of the M1 and M2 muscarinic acetylcholine receptor/G-protein complexes. *Science*. **364**, 552–557 (2019).

49. H. Liu, J. Hofmann, I. Fish, B. Schaake, K. Eitel, A. Bartuschat, J. Kaindl, H. Rampp, A. Banerjee, H. Hübner, Structure-guided development of selective M3 muscarinic acetylcholine receptor antagonists. *Proc. Natl. Acad. Sci.* **115**, 12046–12050 (2018).

50. D. Yuan, Z. Liu, J. Kaindl, S. Maeda, J. Zhao, X. Sun, J. Xu, P. Gmeiner, H.-W. Wang, B. K. Kobilka, Activation of the α 2B adrenoceptor by the sedative sympatholytic dexmedetomidine. *Nat. Chem. Biol.* **16**, 507–512 (2020).

51. Y. Peng, J. D. McCorvy, K. Harpsøe, K. Lansu, S. Yuan, P. Popov, L. Qu, M. Pu, T. Che, L. F. Nikolajsen, 5-HT2C receptor structures reveal the structural basis of GPCR polypharmacology. *Cell*. **172**, 719–730 (2018).